Update of the EST Science Requirements Document

Review on the status of the chapter

Scattering Physics and Hanle-Zeeman diagnostics

Science Advisory Group
SG7

Luca Belluzzi (IRSOL, Switzerland)
Alex Feller (MPS, Germany)
Javier Trujillo Bueno (IAC, Spain)

with contributions from
Rafael Manso Sainz (MPS, Germany)

EST Science Meeting - Giardini Naxos, Italy, 11-15 June 2018

Introduction

TOPIC

The physics and diagnostic capabilities of scattering polarization

CONTENTS

Observing Programs (OPs) focused on scattering polarization signals of interest because of:

- **diagnostic potential** (Hanle effect)
- **physics involved** (scattering / atomic physics)

All these OPs involve **common observational and instrumental requirements**:

- **high polarimetric sensitivity** ($10^{-3} – 10^{-5}$)
- interest to also perform observations **close to the limb or off-limb** (use of AO more difficult)
- simultaneous observation of different lines (e.g., **differential Hanle effect**)
- observation of spectral lines generally not used for Zeeman diagnostics

Structure of the chapter

1. OPs for investigating the **small-scale magnetism of the quiet solar photosphere** via the Hanle effect in atomic and molecular lines

2. OPs for investigating the **magnetism of the chromosphere** via the combined action of Hanle, Zeeman, and magneto-optical (MO) effects

3. OPs of interest for deepening our understanding of the **physics of scattering polarization**

All the proposed OPs require:

- high polarimetric sensitivity

- high spectral resolution

Today, achieving such requirements generally implies to **completely or strongly sacrifice spatial and temporal resolutions.**

Proposed OPs aim at exploiting EST for combining high polarimetric sensitivity and spectral resolution with high spatio-temporal resolution.

Optimal temporal and spatial sampling
(by Alex Feller)

The number of photons collected in a single pixel is

$$N = (S/N)^2 = \Phi \Delta\lambda \, \Delta x^2 \, \Delta t \qquad (1)$$

(Assumption: measurement error dominated by Poisson-distributed photon noise)

Spatial and temporal resolutions are coupled by a characteristic **solar evolution speed**:

$$\Delta x = v \Delta t \qquad (2)$$

The **optimal temporal sampling** (cadence) to reach a given S/N is therefore

$$\Delta t = \left(\frac{(S/N)^2}{\Phi \, \Delta\lambda \, v^2} \right)^{1/3} \qquad (3)$$

The **optimal spatial sampling** is then given by (2)

If the spatial sampling is lower than this optimum value, the decreased photon flux per pixel leads to integration times which exceed the timescale of solar evolution at the given spatial sampling, leading to a **smearing of the observed solar scene**.

Observing Programs (OPs)

1) Small-scale magnetism of the quiet solar photosphere

OP 1.1 – Detection of spatial fluctuations at *sub-granular scales* of the scattering polarization signal of the SrI 4607 Å line

OP 1.2 – Detection of spatial fluctuations at *granular scales* of the scattering polarization signal of the C_2 5140 Å lines

OP 1.3 – Detection of spatial fluctuations at *granular scales* of the scattering polarization signal of TiI a ^5F – y ^5F multiplet at 4530 Å

2) Magnetism of the chromosphere

OP 2.1 – Detecting spatial and temporal variations of the scattering polarization signal of Ca I 4227 Å from the core to the wings

OP 2.2 – Detecting spatial fluctuations of the line-core scattering polarization signal of the Ca II K line at 3934 Å

OP 2.3 – *CaII IR triplet (8498, 8542, 8662 Å)*

OP 2.4 – *OI triplet (7771, 7774, 7775 Å)*

3) Physics of scattering polarization

OP 3.1 – Investigate spatial and temporal variability of the “enigmatic” scattering polarization signal of the Na I D_1 line at 5896 Å

Small-scale magnetism of the quiet solar photosphere

PHYSICAL SCENARIO

The quiet solar photosphere is permeated by small-scale (< 1 arcsec) magnetic fields which strongly interact with turbulent convection.

- Ubiquitous → may play a major role in solar activity and **total magnetic flux**
- May encode information about existence and influence of **local dynamo processes**

DIAGNOSTIC TOOL

Hanle effect

(sensitive to fields tangled on spatial scales even smaller than the resolution element)

Issues:

- Need of a “zero-field” reference value (when using a single line)
- Disentangling Hanle effect from other symmetry breaking phenomena and collisional depolarization

Solutions:

- Comparison with theoretical computations in 3D simulations of the solar photosphere
  e.g., SrI 4607 Å (Trujillo Bueno et al. 2004, Trujillo Bueno & Shchukina 2007)

- Differential Hanle effect techniques
  e.g., C_2 (Trujillo Bueno 2003, Trujillo Bueno et al. 2004, Berdyugina & Fluri 2004, Kleint et al. 2010)
  MgH (Asensio Ramos & Trujillo Bueno, 2005)
  Ti I (Manso Sainz et al. 2005)

Small-scale magnetism of the quiet solar photosphere

Sr I 4607

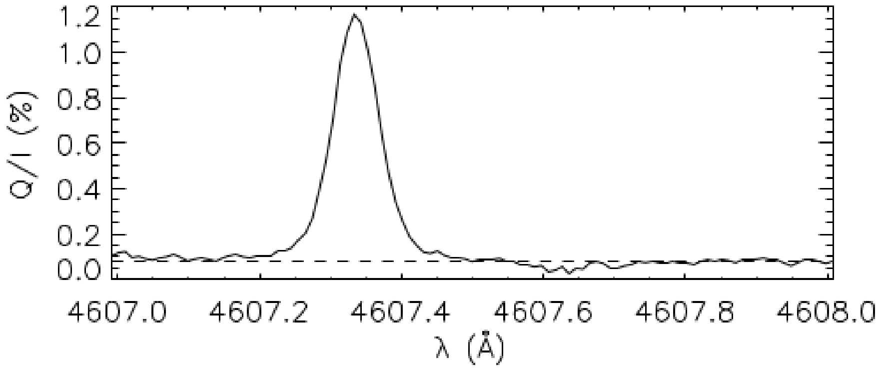

Gandorfer (2002) "The Second Solar Spectrum"

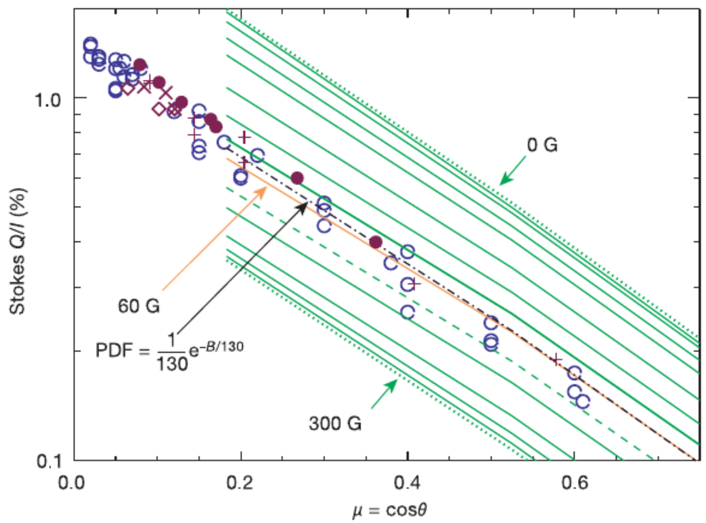

Trujillo Bueno et al. (2004)

C_2 5140

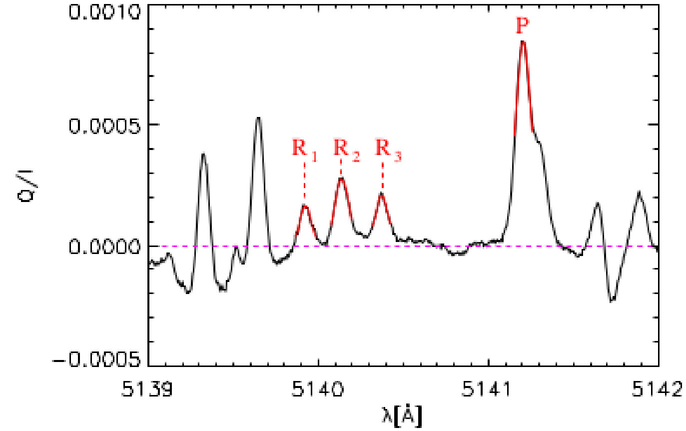

Ramelli et al. (in press)

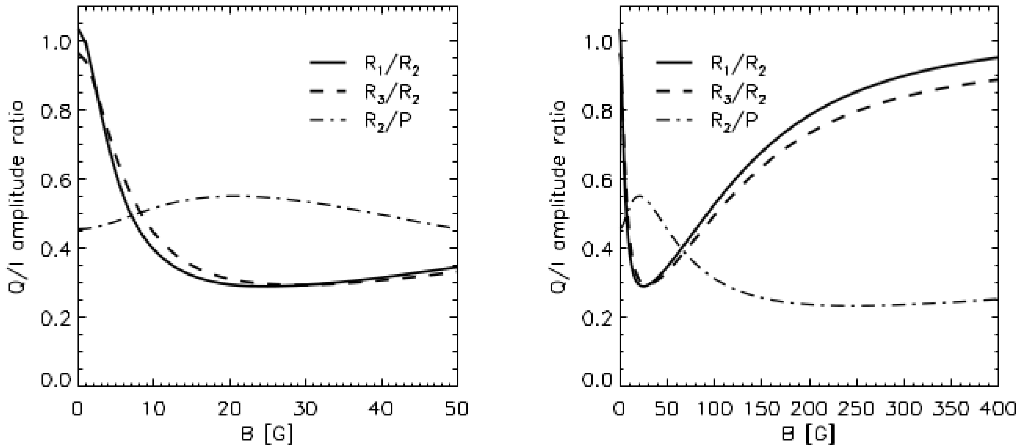

Kleint et al. (2010)

Isotropic, single-valued field B ≈ 60 G

(Trujillo Bueno et al. 2004)

Isotropic, single-valued field B < 10 G

(Trujillo Bueno 2003; Trujillo Bueno et al. 2004; Berdyugina and Fluri 2004, Kleint et al. 2010)

Small-scale magnetism of the quiet solar photosphere

How to explain this disagreement?

Previous results obtained considering observations at **low spatial resolution** (no distinction between granular and intergranular regions)

From numerical simulations it is found that (Trujillo Bueno 2003)

- signals of the **molecular lines** come mainly from the **upflowing granular regions**
- signal of **SrI line** has contributions from both **granular and intergranular regions**

To explain the SrI and C_2 observations (Trujillo Bueno et al. 2004):

a) intergranular plasma with $< B > > 200$ G

b) granular cell centers with $< B > \sim 10$ G

Hanle effect evidence for a fluctuating "hidden" (unresolved) field

Great scientific interest to observe scattering polarization and the Hanle effect at sub-granular spatial scales

OBSERVATIONAL GOAL FOR 4m-CLASS TELESCOPES

Small-scale magnetism of the quiet solar photosphere

THEORETICAL PREDICTIONS

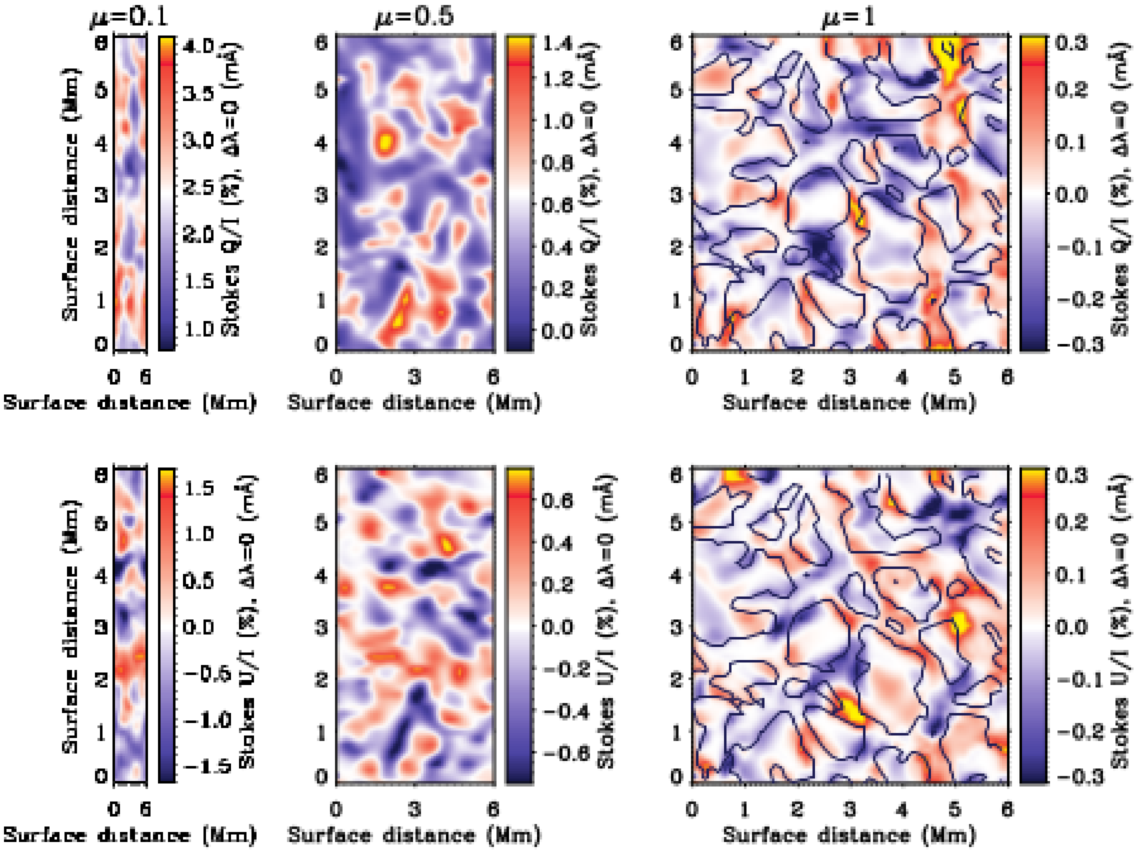

Synthetic scattering polarization signals in the SrI 4607 line calculated in a 3D hydro-dynamical model (Trujillo Bueno & Shchukina, 2007)

No magnetic fields

- Horizontal inhomogeneities produce **measurable signals also at disk-center.** The Q/I and U/I signals have positive and negative values, and fluctuate horizontally with a sub-granular pattern
- Approaching the limb, the amplitude of the fluctuations increases, and Q/I fluctuates around a non-zero value

Small-scale magnetism of the quiet solar photosphere

THEORETICAL PREDICTIONS

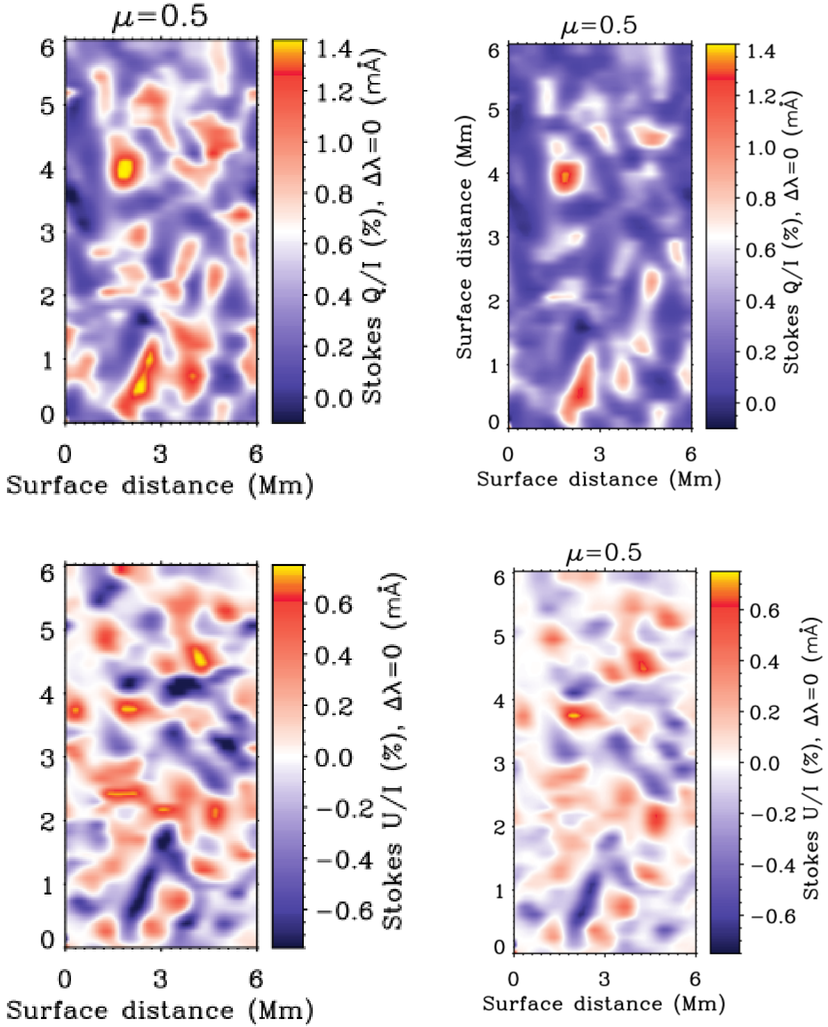

Synthetic scattering polarization signals in the SrI 4607 line calculated in a 3D hydro-dynamical model (Trujillo Bueno & Shchukina, 2007)

B=0

Isotropic tangled field

B=15 G (granular regions)

B=300G (intergranular lanes)

OP 1.1 - Detecting spatial fluctuations at sub-granular scale of scattering polarization in the SrI 4607 Å line

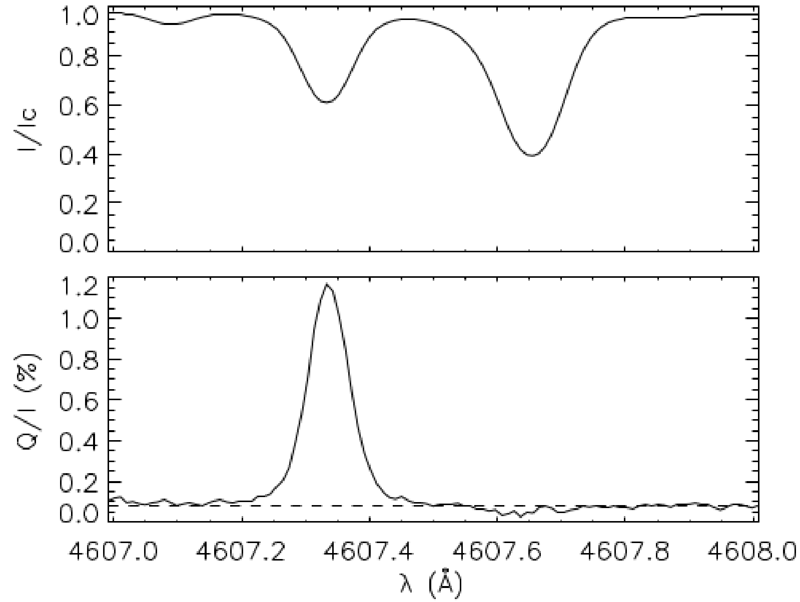

Limb observation (μ=0.1) spatially averaged along the slit (Gandorfer, 2002)

THEORETICAL MODELING

- 2-level atom
- CRD
- need of accurate collisional depolarization rates

DIAGNOSTIC POTENTIAL

- Strong scatter. polar. signal
- $B_H = 23$ G

Narrow-band filter (NB1)

Wavelengths	Sr I 4607.4 Å, Fe I 4607.6 Å	
Polarimetry	Full Stokes	
Polarim. sensitivity	$3.3 \cdot 10^{-4}$ (3-σ detect. of fluct. of 10^{-3})	
Polarim. S/N	$3 \cdot 10^3$	
Spectral FOV	1 Å	
Spectral sampling	25 mÅ/pix	20 mÅ/pix
Spectral samples	3 samples: Sr I line center, Fe I line center, continuum	7 samples: 3 Sr I, 3 Fe I, 1 continuum
Spatial FOV	10 ″ × 10 ″	
Spatial resolution	0.2 ″	0.1 ″
Cadence[(1)]	10 s	5 s
Opt. cadence[(2)]	8.4 s ($\mu = 0.1$)	9.1 s ($\mu = 0.1$)
Opt. spatial sampl.[(2)]	0.08 ″/pix ($\mu = 0.1$)	0.09 ″/pix ($\mu = 0.1$)

OP 1.2 – Detection of spatial fluctuations at granular scales of scattering polarization in C_2 lines at 5140 Å

Observation:
IRSOL telescope (45cm aperture)
ZIMPOL-III

Position: limb (mu=0.1)
Integration time: 15 – 20 min
Signal averaged across 20`` – 30``

Ramelli et al. (in press)

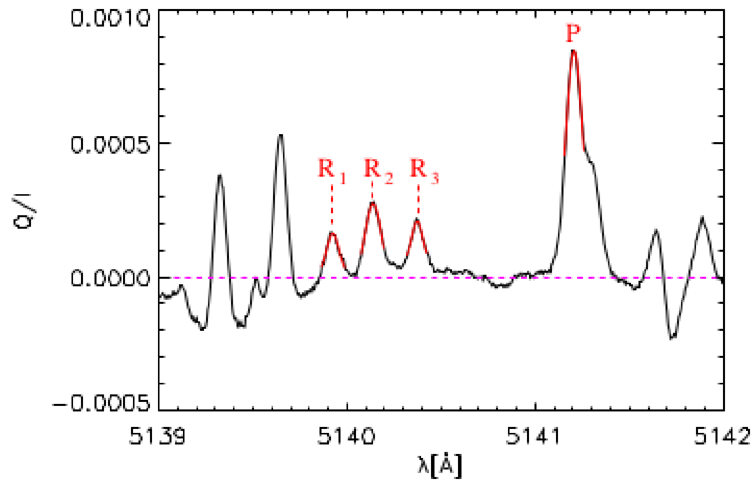

DIAGNOSTIC POTENTIAL

- Differential Hanle effect
  $B_H(R_1, R_3) = 4$ G
  $B_H(R_2) = 40$ G
- Weak signals

Spectrograph (SP)

Wavelengths	C_2 5140 Å	
Polarimetry	Full Stokes	
Polarim. sensitivity	$3.3 \cdot 10^{-5}$ (3-σ detect. of fluct. of 10^{-4})	$1.7 \cdot 10^{-5}$ (3-σ detect. of fluct. of $5 \cdot 10^{-5}$)
Polarim. S/N	$3 \cdot 10^4$	$6 \cdot 10^4$
Spectral FOV	3 Å	
Spectral resolution	20 mÅ	
Spatial FOV	$10'' \times 10''$	
Spatial resolution	$0.5''$	
Cadence(1)	26 s	
Opt. cadence(2)	32 s ($\mu = 0.1$)	50 s ($\mu = 0.1$)
Opt. spatial sampl.(2)	$0.3''$/pix ($\mu = 0.1$)	$0.5''$/pix ($\mu = 0.1$)

OP 1.3 – Detection of spatial fluctuations at granular scales of scattering polarization in the Ti I a ^5F – y ^5F multiplet (4530 Å)

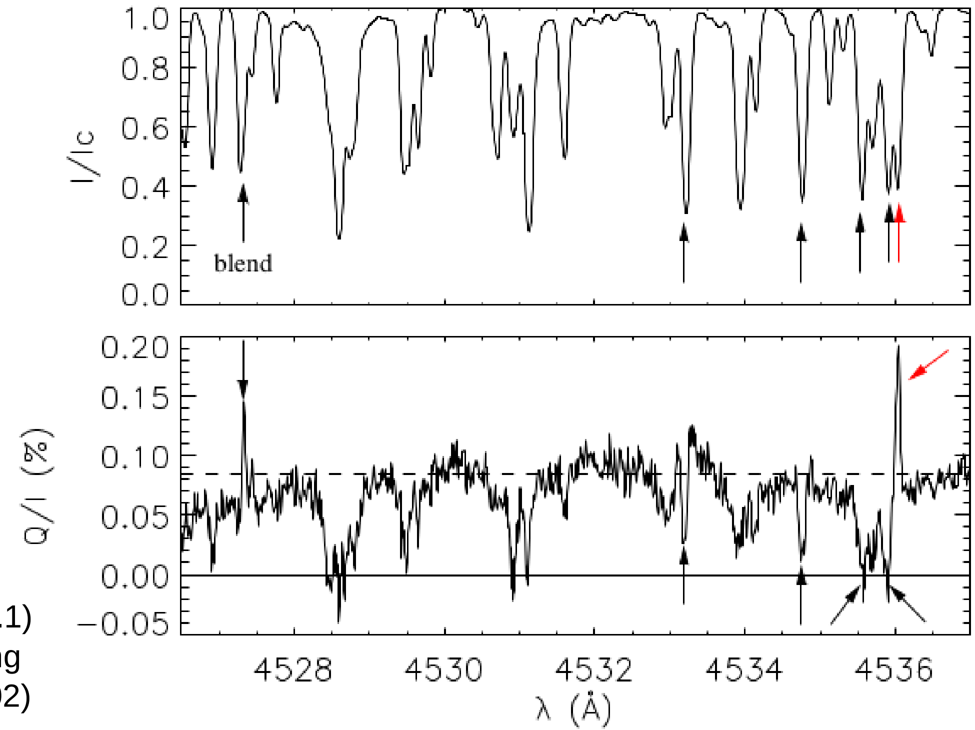

Limb observation (μ=0.1) spatially averaged along the slit (Gandorfer, 2002)

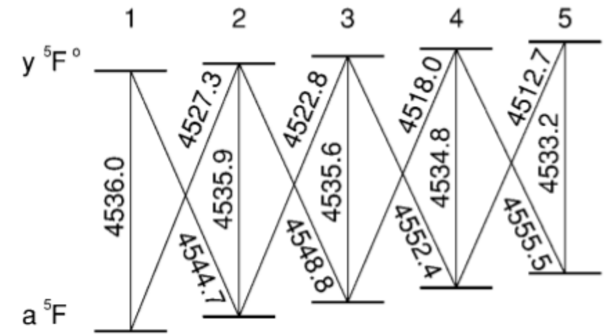

DIAGNOSTIC POTENTIAL

- Differential Hanle effect (line at 4536.04 Å insensitive to magn. field)
- Six lines between 4527 and 4537 Å
- B_H = 8 – 12 G

(see Manso Sainz et al. 2004)

Spectrograph (SP)

Wavelength	4530 Å	
Polarimetry	Full Stokes	
Polarim. sensitivity	$3.3 \cdot 10^{-5}$ (3-σ detect. of fluct. of 10^{-4})	
Polarim. S/N	$3 \cdot 10^4$	
Spectral FOV	10 Å	
Spectral resolution	20 mÅ	
Spatial FOV	10 ″ × 10 ″	
Spatial resolution	0.5 ″	
Cadence$^{(1)}$	26 s	
Opt. cadence$^{(2)}$	50 s ($\mu = 0.1$)	
Opt. spatial sampl.$^{(2)}$	0.5 ″/pix ($\mu = 0.1$)	

Magnetism of the solar chromosphere

Well established diagnostic techniques not available yet

Standard approach:

- **Identify suitable observables** sensitive to the chromospheric magnetic field
- Perform **observations** of such observables
- Infer the desired information by **confronting the observations with the results of theoretical calculations** in realistic simulations of the solar atmosphere

Hanle effect has great potential because:

- Sensitive to **weaker fields** than those that can be investigated via the Zeeman effect
- Sensitive to fields with **opposite polarities below the resolution element**
- Does **not depend on the Doppler width** of the line: it can also be applied where the temperature increases, and from the IR to the UV (where signals are generally larger and density of spectral lines is larger – multi-line diagnostics)

$$V_{\text{Zeeman}} \sim R \qquad R = \frac{\Delta\lambda_B}{\Delta\lambda_D} \sim \frac{\lambda B}{\sqrt{T}}$$

$$Q_{\text{Zeeman}}, U_{\text{Zeeman}} \sim R^2$$

Observational issue for Hanle-Zeeman diagnostics of chromospheric fields:

- **high polarimetric sensitivity required**
- **low photon flux available** (information encoded in the core of strong spectral lines)

LARGE APERTURE TELESCOPES NEEDED

OP 2.1 – Detecting spatial and temporal fluctuations of the scattering polarization signal of Ca I 4227 Å from the core to the wings

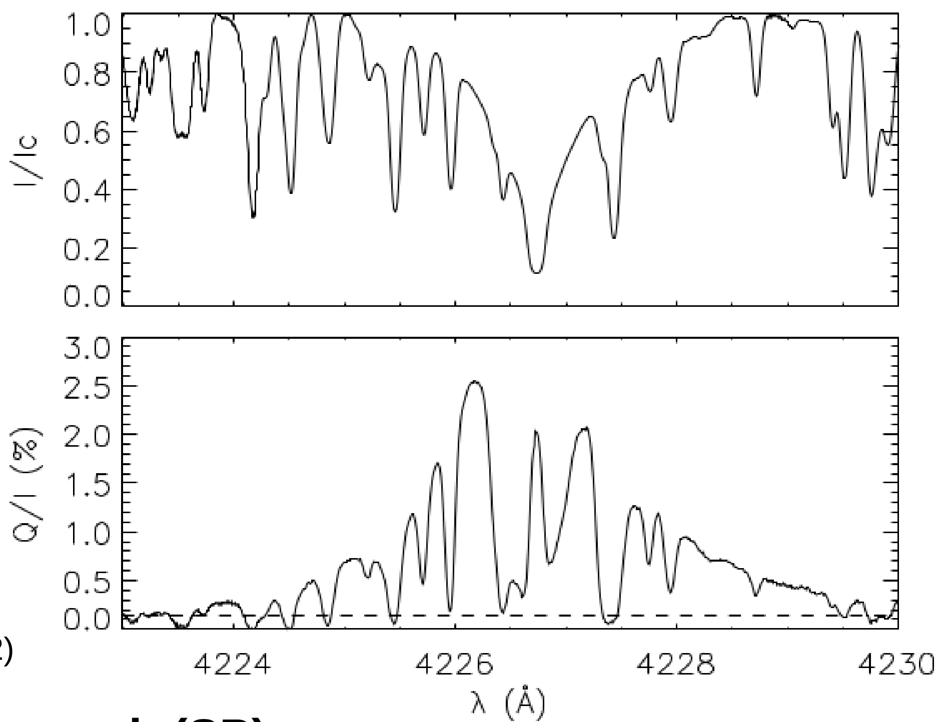

Limb observation (μ=0.1) spatially averaged along the slit (Gandorfer, 2002)

THEORETICAL MODELING

- 2-level atom + PRD effects

(Anusha et al. 2011, Supriya et al. 2014, Sampoorna et al. 2009, Alsina et al. 2018)

DIAGNOSTIC POTENTIAL

Line center peak (low chromosph.)
→ Hanle effect (B_H = 25G)

Wing lobes (photosphere)
→ MO effects (10G)

(see Alsina Ballester et al., 2018)

OBSERVATIONS

Spatial fluctuations of Q/I and U/I detected over scales of about 10``

(Bianda et al. 2011)

Spectrograph (SP)

Wavelength	4227 Å	
Polarimetry	Full Stokes	
Polarim. sensitivity	$3.3 \cdot 10^{-4}$ (3-σ detect. of fluct. of 10^{-3})	
Polarim. S/N	$3 \cdot 10^3$	
Spectral FOV	6 Å	
Spectral resolution	20 mÅ	
Spatial FOV	$1' \times 1'$	
Spatial resolution	1 ″	
Cadence[(1)]	15 s	
Opt. cadence[(2)]	12 s ($\mu = 0.1$)	
Opt. spatial sampl.[(2)]	0.4 ″/pix ($\mu = 0.1$)	

OP 2.2 – Detecting spatial and temporal fluctuations of the line-center scattering polarization signal of the Ca II K line

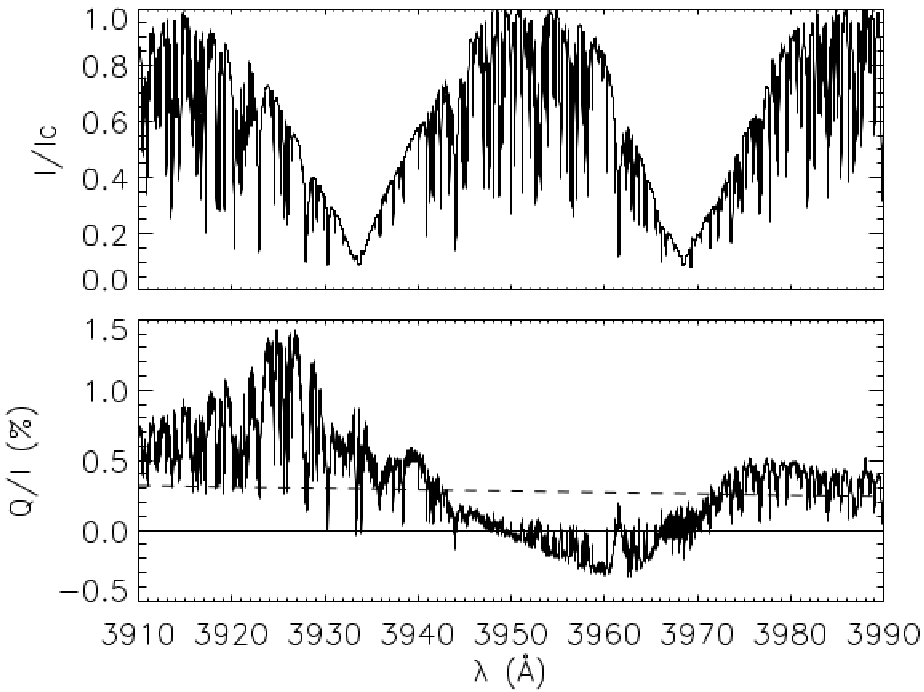

Limb observation (μ=0.1) spatially averaged along the slit (Gandorfer, 2002)

THEORETICAL MODELING

- 5-level (3-term) model atom

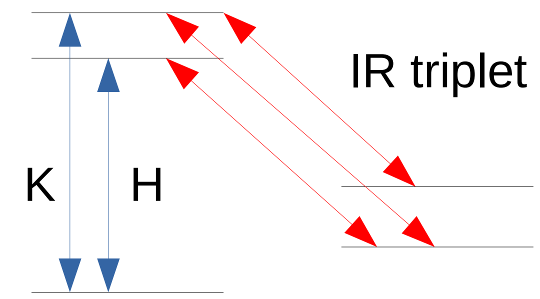

- PRD + J-state interference

New theoretical frameworks available

- Casini et al. (2014)
- Casini & Manso Sainz (2016)
- Casini et al. (2016, 2017)
- Bommier (2016, 2017)

Numerical modeling

- del Pino Aleman et al. (in preparation)

OP 2.2 – Detecting spatial and temporal fluctuations of the line-center scattering polarization signal of the Ca II K line

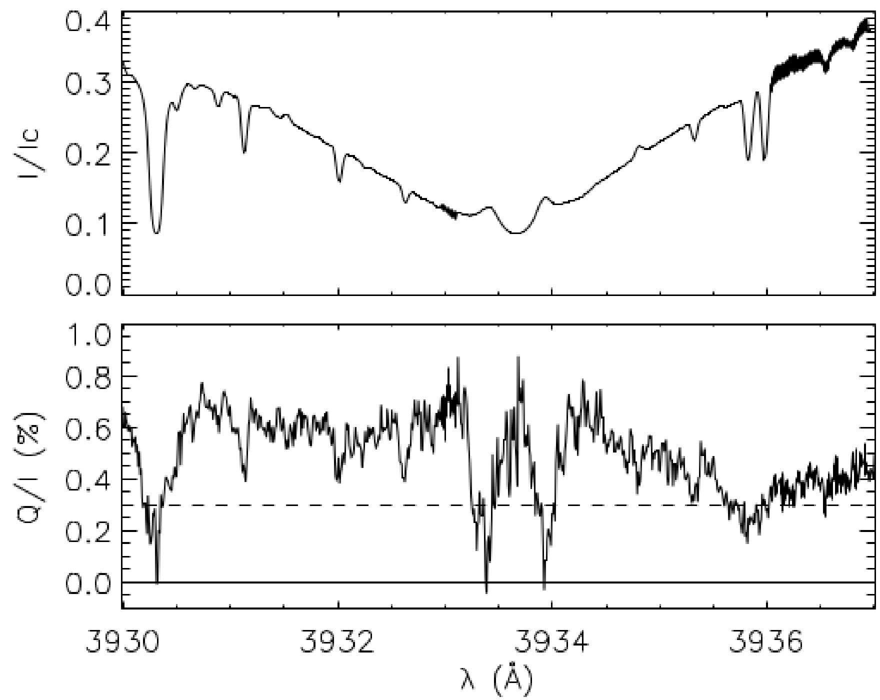

Limb observation (μ=0.1) spatially averaged along the slit (Gandorfer, 2002)

DIAGNOSTIC POTENTIAL

Core of CaII K forms 200-300km below the TR

Line-center Q/I peak sensitive to the Hanle effect (B_H= 12 G)

Wing signals sensitive to MO effects for fields as weak as 20G

V/I dominated by longitudinal Zeeman effect for B > 10G

Spectrograph (SP)

Wavelength	3934 Å	
Polarimetry	Full Stokes	
Polarim. sensitivity	$3.3 \cdot 10^{-4}$ (3-σ detect. of fluct. of 10^{-3})	
Polarim. S/N	3000	
Spectral FOV	10 Å	
Spectral resolution	20 mÅ	
Spatial FOV	$1' \times 1'$	
Spatial resolution	1 $''$	
Cadence(1)	7 s	
Opt. cadence(2)	15 s (μ = 0.1)	
Opt. spatial sampl.(2)	1.0 $''$/pix (μ = 0.1)	

OPs of interest for investigating the physics of scattering

Solid understanding of the (complex!) physics of scattering polarization is required in order to fully exploit its diagnostic potential.

The theoretical interpretation of the rich variety of signals shown by the Second Solar Spectrum has played a key role in this sense.

"Enigmatic" signals of the Second Solar Spectrum have revealed to be the signatures of interesting physical phenomena taking place at the atomic level, which cannot be observed in laboratory plasmas

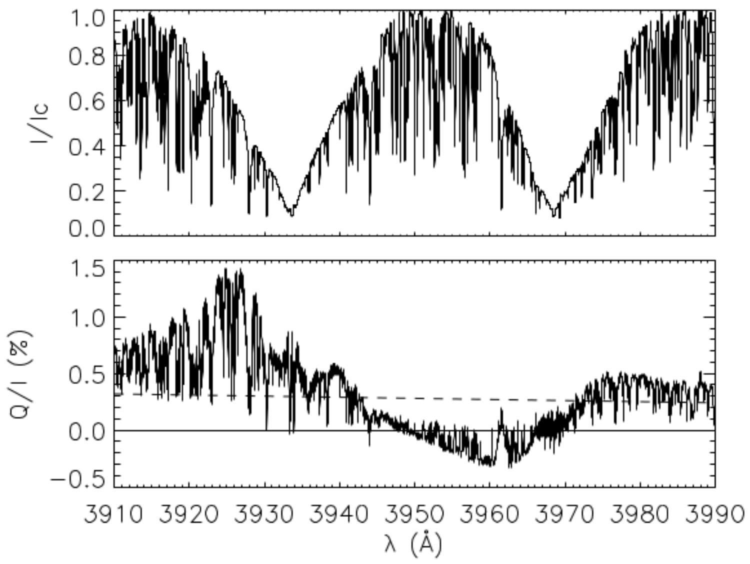

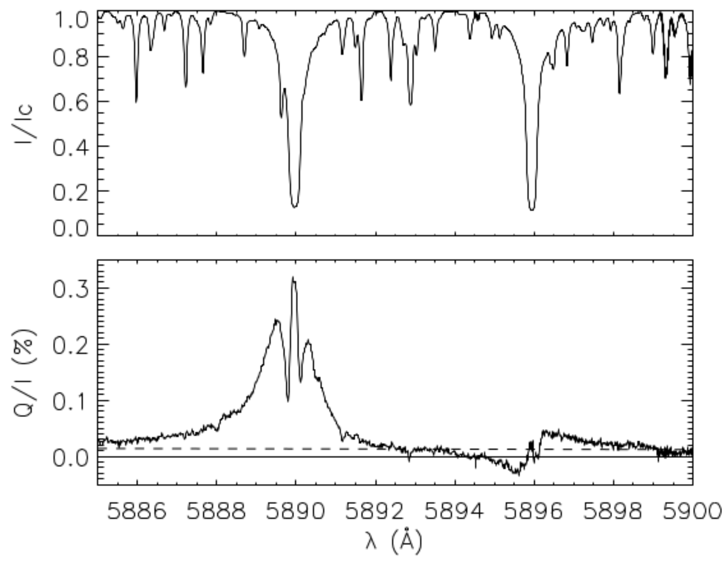

Sign reversal: observational signature of quantum interference between different J-levels (Stenflo, 1980)

OP 3.1 – Investigate spatial and temporal variability of the "enigmatic" scattering polarization signal of the Na I D_1 line

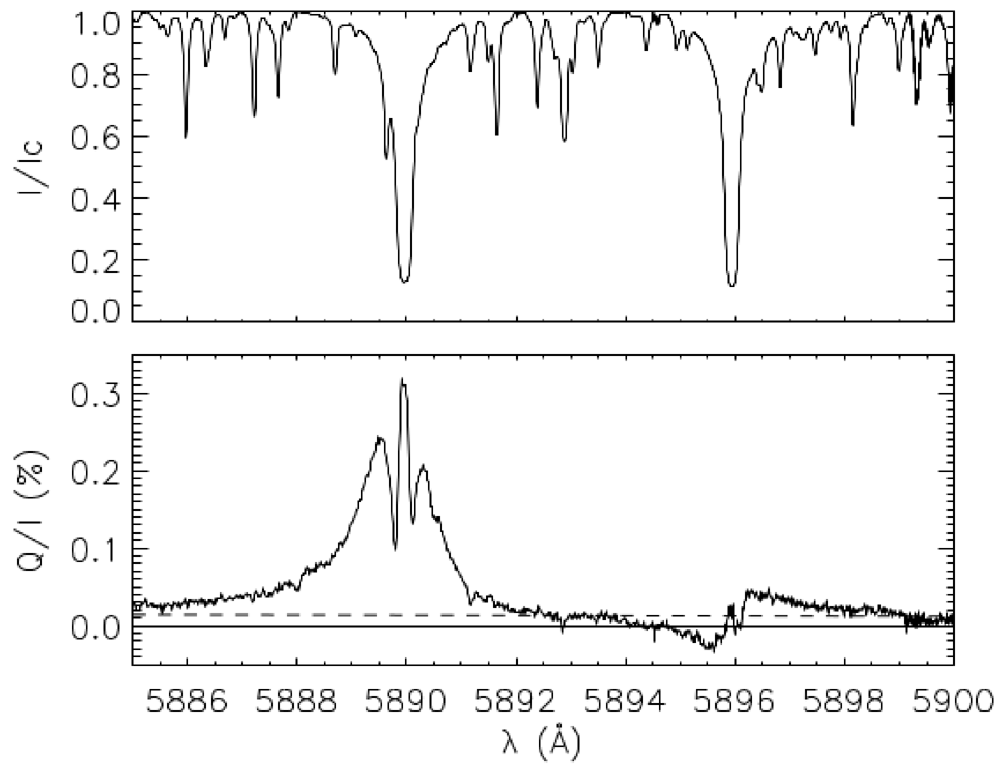

Limb observation (μ=0.1) spatially averaged along the slit (Gandorfer, 2002)

THEORETICAL MODELING

- 2-term atom
- Hyperfine structure
- PRD effects

OP 3.1 – Investigate spatial and temporal variability of the "enigmatic" scattering polarization signal of the Na I D_1 line

Observation:
IRSOL (45cm)
ZIMPOL-III

Position: north limb (mu=0.1)
Integration time: 15min
Signal averaged across 30``
Spectr. res. ~ 10mA

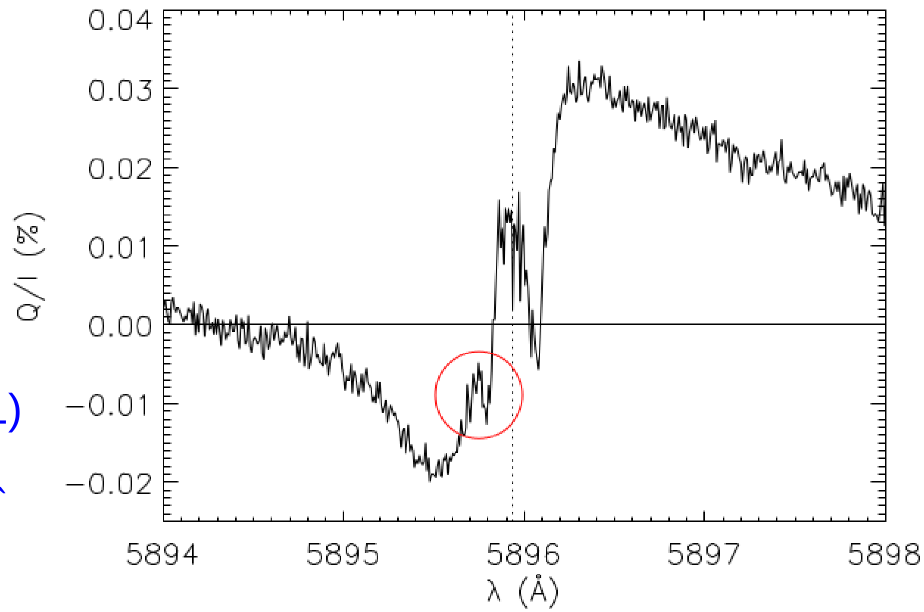

THEORETICAL MODELING

Line-core signal obtained when small variations of the anisotropy of the chromospheric radiation, over spectral intervals as small as the HFS splitting, are taken into account

(Belluzzi & Trujillo Bueno 2013, Belluzzi et al. 2015)

Spectrograph (SP)

Wavelength	5896 Å	
Polarimetry	Full Stokes	
Polarim. sensitivity	$3.3 \cdot 10^{-5}$ (3-σ detect. of fluct. of 10^{-4})	$1.7 \cdot 10^{-5}$ (3-σ detect. of fluct. of $5 \cdot 10^{-5}$)
Polarim. S/N	3×10^4	6×10^4
Spectral FOV	10 Å	
Spectral resolution	20 mÅ	10 mÅ
Spatial FOV	$1' \times 1'$	
Spatial resolution	1 ″- 2 ″	
Cadence(1)	15-30 s	
Opt. cadence(2)	27 s ($\mu = 0.1$)	53 s ($\mu = 0.1$)
Opt. spatial sampl.(2)	0.9 ″/pix ($\mu = 0.1$)	1.8 ″/pix ($\mu = 0.1$)